bringing the H_2CO dipole moment in better alignment with the charge of HOH_2^+.

Examination of the effects of motion of the proton-acceptor group out of the plane of the imine group upon the transfer energetics points out markedly different behavior between the imine and amine. Rather than stabilizing the NH--N configuration as is observed in $(H_3NH--NH_3)^+$, this out-of-plane distortion preferentially stabilizes $(H_2CHN--HNH_3)^+$. This apparent anomaly is attributed to the attractive electrostatic interaction between the charge of HNH_3^+ and the negative out-of-plane component of the quadrupole moment of H_2CNH, a feature which acts also to diminish the energy barrier to proton transfer. Very similar distinctions apply to the O analogues carbonyl and hydroxyl.[28]

With particular regard to the proton transfer energy barriers, in-plane distortions of N bases lead to drastic increases, in contrast to the O bases where small reductions are observed. In the case of out-of-plane distortions, the primary factor is the hybridization of the proton-donor molecule: the barrier increases observed for the sp^2 planar carbonyl and imine groups are several times smaller than for the hydroxyl and amine groups with their pyramidal sp^3 structure.

We have elucidated here a number of general rules concerning the proton-transfer reaction. These rules may provide insights into a number of poorly understood chemical and biological processes. For example, it is clear from the concepts developed here that the deprotonation of the imine group of the bacteriorhodopsin Schiff base could be greatly facilitated if the proton-accepting group were positioned along the direction of the N lone pair but was turned so that its own dipole moment was pointing away from the Schiff base nitrogen. Further stabilization of the deprotonated state of the Schiff base would result from displacement of the proton-accepting group out of the imine plane.

(28) The results for the carbonyl and imine are essentially identical if the out-of-plane angle ϕ is defined relative to the lone pairs of these groups. However, if ϕ is defined relative to the C=O axis of the carbonyl, out-of-plane distortion leads to a small increase in ΔE, due to the nonlinearity of the H bond in the $(H_2COH--OH_2)^+$ configuration prior to the distortion.

Dynamic Jahn–Teller Effects in CH4+. Location of the Transition Structures for Hydrogen Scrambling and Inversion

M. N. Paddon-Row,*[†§] D. J. Fox,[†] J. A. Pople,*[†] K. N. Houk,*[‡] and D. W. Pratt*[‡⊥]

Contribution from the Departments of Chemistry, Carnegie-Mellon University, Pittsburgh, Pennsylvania 15213, and the University of Pittsburgh, Pittsburgh, Pennsylvania 15260. Received June 10, 1985

Abstract: The ground state potential energy surface of CH_4^+ is explored by ab initio molecular orbital theory. In agreement with previous studies, Jahn–Teller distortion of the T_d structure to a C_{2v} structure results in stabilization. Computation of harmonic frequencies for this structure shows $CH_2D_2^+$ to have lowest zero-point energy with two short CD bonds and two long CH bonds. This provides an interpretation of the recent observation that $CH_2D_2^+$ has an EPR spectrum characteristic of such a species. Two C_s transition states for interconverting equivalent C_{2v} structures of CH_4^+ (or CD_4^+) with permuted hydrogens are also found. The lower energy transition state has a small activation energy that is low enough (1–3 kcal/mol) to permit tunneling between six of these structures, making the four hydrogens in CH_4^+ (or CD_4^+) equivalent in EPR experiments, as observed. The second transition state requires higher activation (12–15 kcal/mol) and permits inversion of the pseudotetrahedral C_{2v} form and hence interconversion of all twelve equivalent structures. The low energy for this process suggests that homochiral alkane radical cations should racemize at moderately low temperatures.

Nearly 50 years have elapsed since the discovery by Jahn and Teller of their now celebrated theorem demonstrating the intrinsic geometric instability of orbitally degenerate electronic states.[1] Electron paramagnetic resonance (EPR) spectroscopy has played a central role in revealing some of the static and dynamic consequences of this theorem. The first unambiguous experimental evidence for the Jahn–Teller effect (JTE) was derived from an EPR study of Cu^{2+} in a zinc fluorosilicate crystal at different temperatures.[2] Subsequently, many other systems exhibiting the JTE have been probed with this technique.[3] One of the most remarkable recent examples is the work of Knight et al.[4] on the methane radical cation, CH_4^+, and its deuterated derivatives, in which electron loss from the triply degenerate t_2 orbital of methane can lead to C_{2v}, D_{2d}, and C_{3v} JT-type distortions.

The EPR spectrum of CH_4^+, produced by three independent techniques and examined in a neon matrix at 4 K, is an approximately isotropic quintet with $a_H = 54.8$ G and $g_{iso} = 2.0029$, suggesting the existence of four magnetically equivalent protons on the EPR time scale. This is consistent with an average D_{2d} geometry for the parent ion. However, the corresponding spectrum of $CH_2D_2^+$ exhibits a nearly isotropic triplet of quintets with $a_H = 121.7$ G, $a_D = 2.22$ G, and $g_{iso} = 2.0029$. Multiplication of the D hyperfine splitting (hfs) by the appropriate nuclear g-factor ratio yields a corresponding proton hfs of $a_{H'} = 14.6$ G, suggesting the existence of two pairs of magnetically *in*equivalent "protons" in $CH_2D_2^+$. This is consistent only with a C_{2v} geometry. Comparison of these hfs with those predicted by ab initio CI spin density calculations[5] on CH_4^+ confirms the C_{2v} assignment.

[†] Carnegie-Mellon University.
[‡] University of Pittsburgh.
[§] Present address: Department of Organic Chemistry, The University of New South Wales, Kensington, N.S.W., Australia 2033.
[⊥] Fellow of the J. S. Guggenheim Foundation.

(1) Jahn, H. A.; Teller, E., *Phys. Rev.* **1936**, *49*, 874. Jahn, H. A.; Teller, E. *Proc. R. Soc. (London)* **1937**, *A161*, 220.
(2) Bleaney, B.; Ingram, D. J. E. *Proc. Phys. Soc. (London)* **1950**, *A63*, 408. Abragam, A.; Pryce, M. H. L. *Proc. Phys. Soc. (London)* **1950**, *A63*, 409. Bleaney, B.; Bowers, K. D. *Proc. Phys. Soc. (London)* **1952**, *A65*, 667.
(3) Ham, F. S. In "Electron Paramagnetic Resonance"; Geschwind, S., Ed.; Plenum Press: New York, 1972; p 1. See also: Bersuker, I. B. "The Jahn–Teller Effect and Vibronic Interactions in Modern Chemistry"; Plenum Press: New York 1984.
(4) Knight, L. B., Jr.; Steadman, J.; Feller, D.; Davidson, E. R. *J. Am. Chem. Soc.* **1984**, *106*, 3700.
(5) Feller, D.; Davidson, E. R. *J. Chem. Phys.* **1983**, *80*, 1006.

Dynamic Jahn–Teller Effects in CH₄⁺

J. Am. Chem. Soc., Vol. 107, No. 25, 1985 7697

Table I. Total and Relative Energies[a] of CH_4^+

level[b]	D_{2d} (1)	C_{2v} (2)	C_s (3)	C_s (4)
HF/6-31G*	39.75044 (2.6)[c]	39.75462 (0)[c]	39.75060 (2.5)	39.72880 (16.2)
MP4/6-31G**//6-31G*	39.92074 (3.1)	39.92565 (0)	39.92047 (3.3)	39.90066 (15.7)
same + ZPE	39.88457 (0.7)	39.88562 (0)	39.88338 (1.4)	39.86567 (12.5)
HF/6-31G**	39.76036 (5.4)[c]	39.76896 (0)[c]	39.76109 (4.9)	
MP4/6-31G**//6-31G**		39.92624 (0)	39.92018 (3.8)	
same + ZPE		39.88569 (0)	39.88287 (1.8)	
MP2/6-31G**	39.90229 (3.4)	39.90778 (0)	39.90230 (3.4)	
MP4/6-31G**//MP2/6-31G**	39.92079 (3.5)	39.92632 (0)	39.92079 (3.5)	
same + ZPE	39.88510 (0.7)	39.88626 (0)	39.88458 (1.1)	

[a] Total energies in hartrees (negative signs omitted); energies relative to those of **2** are in kcal/mol and are given in parentheses. [b] Level of energy calculation//level at which geometry was optimized. The MP2 optimizations were full, whereas the MP4 calculations were performed with the frozen core approximation. Imaginary frequencies (two for **1** and one for **3** and **4**) were not included in ZPE calculations. [c] Also reported in ref 8.

On the basis of the observation that the average value $[(a_H + a_H)/2]$ of the "proton" hfs of $CH_2D_2^+$ is 53.6 G, essentially the same as that observed for CH_4^+ (54.8 G), Knight et al.[4] surmised that the geometry of *both* species is, in fact, C_{2v}, that a dynamic JTE or fluxional behavior causes rapid averaging of the proton environments in CH_4^+, yielding the spectrum of a D_{2d} molecule, and that zero-point energy (ZPE) differences might prevent such averaging effects in $CH_2D_2^+$ at 4 K. While this interpretation of the EPR results seemed plausible to us, it was by no means clear why the spectrum of $CH_2D_2^+$ could be assigned to a *single* isomer with the D atoms occupying *only* those positions having a small spin density. We were also intrigued by the possibility that higher level calculations might provide more information about the geometries, vibrational frequencies, and ZPE's of the distorted configurations that correspond to stable minima when the symmetric configuration is unstable as a result of the JT theorem. A successful theoretical resolution of some of these issues is reported here. We also report the location of two different transition states for interconversion of the different C_{2v} structures of CH_4^+.

Early ab initio theoretical work on CH_4^+ favored a D_{2d} "flattened" structure **1**.[6] However, in 1973 a much higher level study by Meyer[7] predicted a C_{2v} form, **2**, with one HCH bond angle ($\angle H_1CH_2 = 56.3°$) much smaller than the other ($\angle H_3CH_4 = 121.9°$). More recent calculations by Bouma, Poppinger, and Radom[8] support this conclusion.

In the present theoretical work (using the GAUSSIAN 82 program[9]), unrestricted Hartree–Fock (HF) calculations were carried out first with the 6-31G* basis and then with 6-31G**, which has polarization functions on all atoms. In addition, some structures were optimized with the second-order Møller–Plesset correlated method, MP2/6-31G**. Geometry optimizations were followed by harmonic frequency calculations which were then used to determine zero-point energies. Finally, some single-point calculations were performed at the fourth-order MP4 level.

Following Bouma et al.,[8] the D_{2d} and C_{2v} symmetry-constrained structures, **1** and **2**, were optimized and subjected to harmonic frequency analysis. Our MP2 optimizations used all orbitals, whereas Bouma et al. performed optimizations with a frozen core approximation in the MP2 expansion.[8] At all levels of theory, the C_{2v} form has lowest energy (Table 1) and is found to be a local minimum (all real frequencies). The D_{2d} structure, on the other hand, has two imaginary frequencies and cannot, therefore, be a minimum on the potential surface.[8] It is also ruled out as a transition state for interconverting equivalent forms.[10]

Geometrical parameters of **1** and **2** at two of the levels used are listed in Table II. The geometries obtained at the 6-31G*

(6) Lathan, W. A.; Hehre, W. J.; Curtiss, L. A.; Pople, J. A. *J. Am. Chem. Soc.* **1971**, *93*, 6377.

(7) Meyer, W. *J. Chem. Phys.* **1973**, *58*, 1017.

(8) Bouma, W. J.; Poppinger, D.; Radom, L. *Isr. J. Chem.* **1983**, *23*, 21.

(9) Binkley, J. S.; Frisch, M.; Roghavachari, K.; DeFrees, D. J.; Schlegel, H. B.; Whiteside, R.; Fluder, E.; Seeger, R.; Pople, J. A. GAUSSIAN 82, Carnegie-Mellon University, Pittsburgh, PA.

(10) Murrell, J. N.; Laidler, K. J. *Trans. Faraday Soc.* **1968**, *64*, 371. McIver, J. W.; Stanton, R. E. *J. Am. Chem. Soc.* **1972**, *94*, 8618. McIver, J. W. *Acc. Chem. Res.* **1974**, *7*, 72.
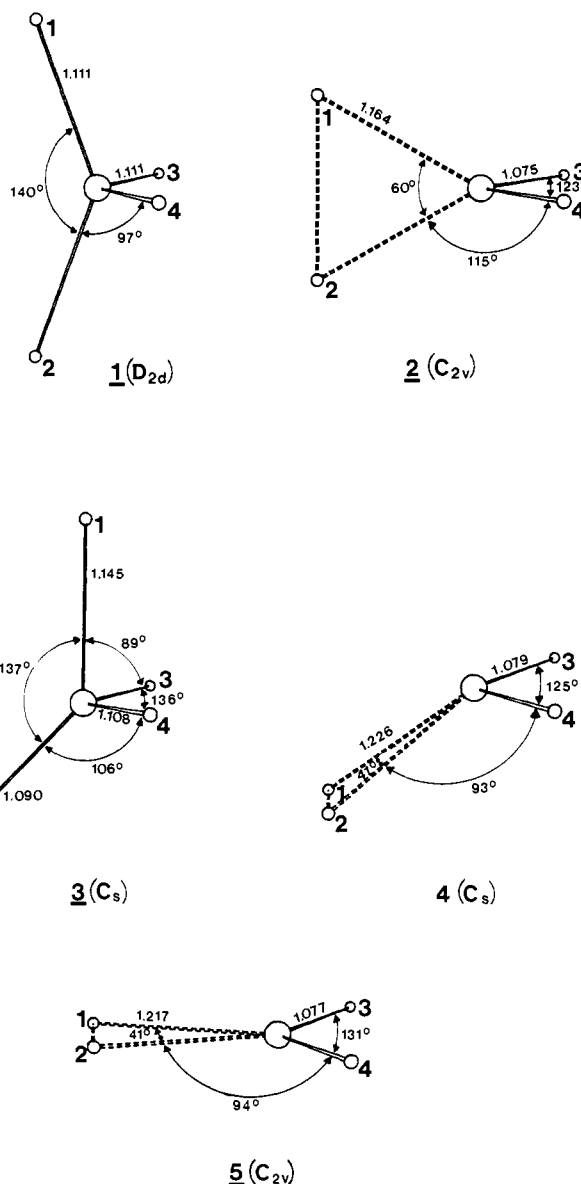
Figure 1. 6-31G* geometries of CH_4^+ radical cations. At the highest levels for which harmonic frequencies were calculated, **1–5** have 2, 0, 1, 1, and 2 imaginary frequencies, respectively. Each structure is drawn so that a plane of symmetry bisects the H_3CH_4 angle. This symmetry plane is tilted forward from the horizontal by 5° in **1–3** and 10° in **4** and **5** to improve visual perspective.

level are shown in Figure 1. For the C_{2v} equilibrium form, **2**, the MP2/6-31G** geometry is very similar to the HF/6-31G* structure, suggesting that correlation effects do not significantly influence the structures of small alkane radical cations.

Table II. Geometries of Stationary Points on the CH_4^+ Surface[a]

	level	1 (D_{2d})[b]	2 (C_{2v})[b]	3 (C_s)	4 (C_s)
CH_1	6-31G*	1.1111	1.1635	1.1455	1.2263
	MP2/6-31G**	1.1139	1.1745	1.1245	
CH_2	6-31G*	1.1111	1.1635	1.0900	1.2263
	MP2/6-31G**	1.1139	1.1745	1.1020	
CH_3	6-31G*	1.1111	1.0750	1.1083	1.0786
	MP2/6-31G**	1.1139	1.0782	1.1123	
CH_4	6-31G*	1.1111	1.0750	1.1083	1.0786
	MP2/6-31G**	1.1139	1.0782	1.1123	
H_1CH_2	6-31G*	140.0	59.0	136.8	40.5
	MP2/6-31G**	141.0	54.6	140.4	
H_1CH_3	6-31G*	96.8	114.5	88.8	92.5
	MP2/6-31G**	95.8	114.2	91.6	
H_1CH_4	6-31G*	96.8	114.5	88.8	135.1
	MP2/6-31G**	95.8	114.2	91.6	
H_2CH_3	6-31G*	96.8	114.5	105.7	135.1
	MP2/6-31G**	95.8	114.2	101.3	
H_2CH_4	6-31G*	96.8	114.5	105.7	92.5
	MP2/6-31G**	95.8	114.2	101.3	
H_3CH_4	6-31G*	140.0	123.0	136.1	124.9
	MP2/6-31G**	141.0	125.0	139.9	

[a] Lengths in angstroms; angles in degrees. [b] Reported in ref 8.

The harmonic vibrational frequencies of CH_4^+, the three possible $CH_2D_2^+$ isomers, and CD_4^+ were calculated at the MP2/6-31G** level. The results are given in Table III along with the ZPE's of each of these species. CH_4^+ has two "short" (s) and two "long" (l) C–H bonds. Therefore, large isotope effects are expected and found. Most relevant to the present discussion are the ZPE's of the three $CH_2D_2^+$ isomers: 21.5, 21.8, and 22.1 kcal/mol^{-1}, respectively. While small, the differences in these values (~ 300 and 600 cal/mol^{-1}) are more than sufficient to guarantee that only one of the three isomers exists in a neon matrix at 4 K, where $RT \sim 10$ cal/mol^{-1}. The unique isomer is the one with deuteriums attached to the short bond positions. Clearly, deuterium "prefers" these positions because the resulting decrease in ZPE is larger than that for the long bond positions, short and relative strong bonds having higher force constants and vibrational frequencies than long ones. The short bonds also have hydrogens in the nodal plane of the principal orbital containing unpaired spin, whereas the long bonds have hydrogens which mix appreciably with this carbon orbital. This accounts for the magnetic inequivalence of the four "protons" in $CH_2D_2^+$.

We conclude, then, that ZPE differences are largely responsible for the fact that $CH_2D_2^+$ exists at sufficiently low temperatures as a stable, distorted configuration of C_{2v} symmetry and, as such, is a classic example of the static Jahn–Teller effect. While such an "isotopically induced" distortion might have been expected, we are unaware of other examples of this effect in the literature.

The situation is qualitatively different in CH_4^+ (and CD_4^+) because all C_{2v} structures have the same ZPE. Thus, a dynamic JTE is expected, providing there is sufficient coupling between the electronic and vibrational degrees of freedom to permit sampling each of the C_{2v} minima within the time frame of the experiment. Clearly, this is the case for CH_4^+ at 4 K in a neon matrix since its single proton hfs is equal to the average value observed for $CH_2D_2^+$.[4] How does this averaging occur?

Intrigued by this question, we have searched the nine-dimensional potential energy surface for suitable transition states using
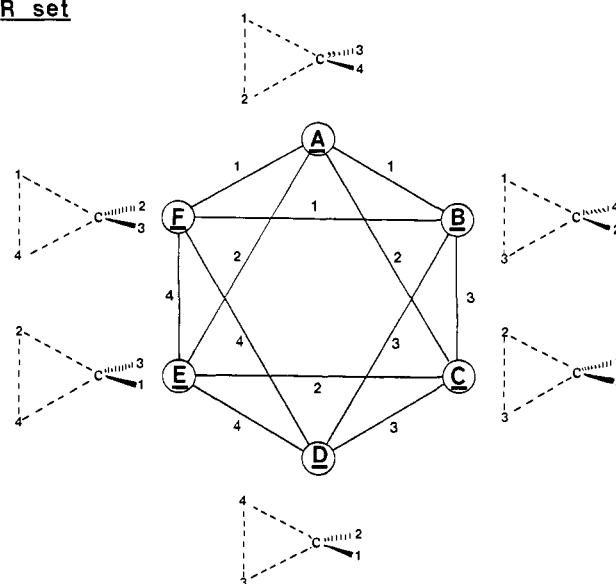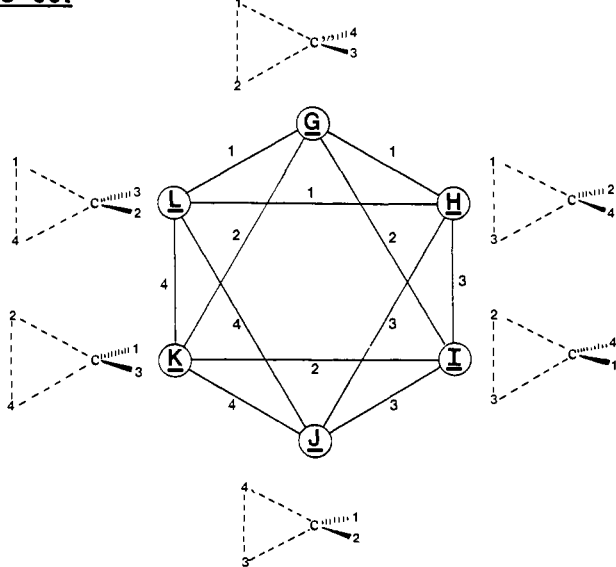

Figure 2. The twelve equivalent hydrogen permutations in C_{2v} CH_4^+ (2). Each number is a hydrogen label. Lines connecting structures represent interconversions via the transition structure, 3. The numbers by each line represent a formal axis of pseudorotation around that bond that remains long in the interconversion. Transition structure 4 formally interconverts A and G, B and H, etc., or the R set (A–F) with the S set (G–L).

the criterion that the force-constant matrix must have one and only one negative eigenvalue. Although initial searches were performed with no symmetry constraints, two transition states,

Table III. Calculated MP2/6-31G** Vibrational Frequencies (cm^{-1}) and Zero-Point Energies (kcal/mol) of the C_{2v} Ground States of CH_4^+, $CH_2D_2^+$, and CD_4^+

		CH_4^+	$CH_1H_1D_sD_s^+$	$CH_1H_sD_1D_s^+$	$CH_sH_sD_1D_1^+$	CD_4^+
	a_1	1265	1020	1068	998	941
		1651	1514	1461	1501	1170
		2694	2318	1834	2000	1965
		3283	2744	3361	3276	2392
	a_2	543	509	454	428	384
	b_1	1370	777	847	1208	1019
		3428	2391	2421	3428	2567
	b_2	952	1206	1218	923	740
		2394	2568	2610	1716	1712
	ZPE	25.1	21.5	21.8	22.1	18.4

Dynamic Jahn–Teller Effects in CH₄⁺
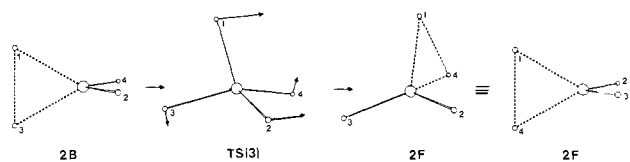
J. Am. Chem. Soc., Vol. 107, No. 25, 1985 7699

Figure 3. Representation of the conversion of **2B** to **2F** via transition structure 3. The arrows on **3** represent the transition vector.

Figure 4. Representation of the conversion of **2A** to **2G** via transition structure 4. The arrows on **4** represent the transition vector.

3 and **4**, were found, both with C_s symmetry. Energies and structural parameters for these are listed in Tables I and II and Figure 1. Calculations on structure **3** were performed at levels up to MP2/6-31G**, whereas those on structure **4** were carried out only at the 6-31G* level since there is no indication of substantial influence of basis sets or correlation effects on energies. A planar C_{2v} structure, **5**, similar to **4** but with two negative eigenvalues, was also located.

The two different transition states, **3** and **4**, correspond to two different dynamic processes which scramble the hydrogens in topologically distinct ways. Numbering these atoms, there are twelve energetically equivalent C_{2v} isomers of CH₄⁺. These are shown in Figure 2. These divide into two subsets, A–F and G–L. A member of the first set is an enantiomer (nonsuperimposable mirror image) of a member of the second set. Each set thus represents an enantiomeric set of pseudotetrahedral CH₄⁺ stereoisomers. Using the usual Cahn–Ingold–Prelog RS notation,[11] with labels 1–4 now representing atom priorities, A–F belong to the **R** set and G–L belong to the **S** set. The transition state **3** connects *A* to *B*, *C*, *E*, or *F*. Starting from A, bonds CH₁ and CH₄ remain long and short, respectively, in the conversion to B. The motion involved in this interconversion via **3** can be considered formally to be a pseudorotation about the long CH₁ bond. By similar motions around one long bond, A can form C, E, or F, but D can be formed from A only by two (or more) pseudorotations via **3**. The numbers along each line connecting structures in Figure 2 designate the long bond around which pseudorotation occurs. Each interconversion could, alternatively, be considered a pseudorotation about the short bond which remains short in the transformation, or about either of the other two bonds. By this mechanism, the six isomers A–F may all be interconverted, thereby resulting in an averaging of their respective hfs if the rate of the exchange is sufficiently fast.

It may be noted that the geometry of the transition state **3** is similar to that of the D_{2d} structure, **1**. Both structures also have nearly identical energies (Table I), but the D_{2d} structure, **1**, has two negative eigenvalues in the force-constant matrix and is therefore avoided by the interconversion of the six C_{2v} structures A to F via **3**. The bond lengths in Figure 1 show the similarities between **1** and **3**. If **1** had been the transition state, then crosshexagon ("para") interconversion, e.g., A → D, would occur in Figure 2. However, the D_{2d} structure, **1**, has two negative force constants and distorts to the lower energy transition structure, **3**, so that only "meta" transformations occur via **3**. The activation energy for this process is quite low. The best results in Table I suggest a classical barrier of 3.5 kcal/mol. Zero-point energy differences between **2** and **3** lower the activation energy to around 1 kcal/mol.[12]

The hydrogen scrambling via **3** is represented in more detail in Figure 3. In order for the labeling of the transition state **TS(3)** in Figure 3 to be the same as that in drawing **3**, the transformation of **2B** to **2F** has been depicted. The arrows on **TS(3)** represent the "transition vector" or hydrogen motions associated with the imaginary frequency representing motion along the reaction coordinate with a negative force constant.[10] H-1, which is closest to H-3 in structure **2A**, moves away from H-3 toward H-4. There is considerable motion of H-2 also. The transition state has C_s
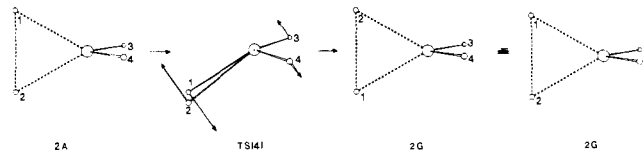
symmetry since H-1 is exactly half-transferred from H-3 to H-4. In TS(3), the plane of symmetry containing atoms H-1, C, H-2 bisects the H-3, C, H-4 angle. Drawing **3** in Figure 1 shows this more clearly.

As the motion toward **3** occurs, the CH bond lengths become more similar than they are in **2** because **3** is not very different from **1** which has four equal CH bond lengths. Nevertheless, transition state **3** has three different types of bonds. In the structure connecting **2B** with **2F** (Figure 3), the bond to H-1 is long in **2B** and **2F** and is also the longest bond in **3**. The bond to H-2 is short in **2B**, **2F**, and **3**. The bond to H-3 is converted from a long to a short bond, while that to H-4 is converted from short to long. In **3**, the bonds to H-3 and H-4 are both intermediate in length, as these atoms trade places.

Conversion of the **R** set to the **S** set (A → G, etc.) cannot occur via **3**. Instead, this interconversion can occur only through the higher energy transition state, **4**. As shown in Figure 1, this structure has all four hydrogens in the same hemisphere centered at carbon. According to the numbering shown, **4** connects the two minima A and G. This path is equivalent to internal rotation about the twofold axis of the C_{2v} structure, thereby interchanging positions 3 and 4. Structure **4** is a nonplanar form related to the planar C_{2v} structure **5** which has two negative eigenvalues in the force constant matrix. Structure **5** is only 0.6 kcal/mol higher in energy than **4** at the 6-31G* level. Rotation about the C_2 axis of **2** would lead directly to **5**, but this is avoided by distortion to **4** which has only one negative eigenvalue. Figure 4 shows the interconversion of **2A** and **2G** via transition state **4**. The transition vector illustrated by the arrows on **4** clearly shows the rotation of the H-1, C, H-2 unit and the H-3, C, H-4 unit in opposite directions.

The activation energy for rearrangement through the transition state **4** is higher than that through **3** (12.5 kcal/mol vs. 1.4 kcal/mol at the MP4/6-31G**//6-31G* + ZPE level). It follows that hydrogen scrambling in CH₄⁺ occurs in two stages. Crossing the barrier through **3** interconverts equivalent isomers *within* the sets A–F and G–L. Crossing **4** at higher energies interconverts isomers *between* the sets, leading to complete access to all forms. The transition state **4** is that for *inversion* of CH₄⁺ when this is regarded as a pseudotetrahedral structure. The barrier for inversion of CH₄⁺ of only 12–15 kcal/mol stands in sharp contrast to methane itself which is calculated to have a barrier to inversion comparable to that required for CH dissociation.[13] At the MP2/6-31G*//6-31G* level, D_{4h} methane is 160 kcal/mol less stable than T_d methane![8] At the 6-31G* level, planar cation **5** is only 13 kcal/mol above the optimum C_{2v} structure, **2**. The low barrier to inversion of CH₄⁺ suggests that homochiral alkane radical cations will readily racemize in fluid solution. The ready generation of such species by γ-irradiation[14] indicates that an experimental test of this prediction could be carried out.[15]

Returning to CH₄⁺, it is clear that the EPR observations[4] only require passage over the barriers corresponding to the transition

(11) Cahn, R. S.; Ingold, C. K.; Prelog, V. *Experientia* **1956**, *12*, 81.

(12) A referee has noted, correctly, that some caution should be used in interpreting the calculated harmonic vibrational frequencies given that the ZPE is a significant fraction of the barrier height. Indeed, the imaginary frequencies associated with both **1** and **3** are very small, suggesting that the potential surface is quite flat in the vicinity of the transition state.

(13) Pople, J. A., unpublished results; see also: Krogh-Jespersen, M.-B.; Chandrasekhar, J.; Wurthwein, E.-U.; Collins, J. B.; Schleyer, P. v. R. *J. Am. Chem. Soc.* **1980**, *102*, 2263.

(14) See, for example: Nunome, K.; Toriyama, Iwasaki, M. *J. Chem. Phys.* **1983**, *79*, 2499. Symons, M. C. R. *Chem. Soc. Rev.* **1984**, *13*, 393 and references therein.

(15) The simplest acyclic chiral hydrocarbons in which this could be observed are 3-methylhexane and 2,3-dimethylpentane. A variety of calculations and experimental data on alkane radical cations indicate the "CC long-bond" structures are favored for these species. Because of this, the pseudo-planar achiral transition structures for racemization may be higher in energy than in CH₄⁺. See ref 8 for extensive alkane radical cation calculations and discussions of experimental and other computational results.

state **3**. But some issues remain unresolved. The most refined calculations give 1.1 kcal/mol for the process A → **3** → B. This is too large to permit crossing by thermal activation at 4 K. Tunneling through the barrier is a distinct possibility since relatively minor hydrogen motions are required. The magnetic inequivalence of the protons in C_{2v} CH_4^+ is about 100 G. Averaging this inequivalence by tunneling would require a rate of penetration of the barrier of at least 3×10^8 s^{-1}. The calculations on $CH_2D_2^+$ impose an upper limit on this frequency of $ZPE(CH_1H_1D_sD_s^+)$ – $ZPE(CH_1H_sD_1D_s^+) \sim 3 \times 10^{12}$ s^{-1}. These limits do not seem unreasonable in view of the barrier height and the known tunneling frequencies associated with other weakly hindered motions (e.g., ~ 500 MHz for methyl rotors).[16] Variable-temperature studies

of the EPR spectra of CH_4^+ and CD_4^+ may reveal changes in the relative intensities of different hyperfine components which could be used to measure the splitting of the ground vibronic level due to tunneling. We also urge similar studies of $CH_2D_2^+$ and other deuterated derivatives to search for other, less stable, isomers and the onset of dynamic behavior.

(16) Clough, S.; Poldy, F. *J. Phys.* **1973**, *C6*, 1953.

Interconversion of μ-Alkylidyne and μ-Alkenyl Diiron Complexes

Charles P. Casey,* Seth R. Marder, and Bruce R. Adams

Contribution from the Department of Chemistry, University of Wisconsin, Madison, Wisconsin 53706. Received June 11, 1985

Abstract: The μ-pentylidyne complex $[(C_5H_5)_2(CO)_2Fe_2(\mu\text{-}CO)_2(\mu\text{-}CCH_2CH_2CH_2CH_3)]^+PF_6^-$ (**3**) rearranged to the μ-pentenyl complex $[(C_5H_5)_2(CO)_2Fe_2(\mu\text{-}CO)(\mu\text{-}\eta^1,\eta^2\text{-}(E)\text{-}CH=CHCH_2CH_2CH_3)]^+PF_6^-$ (**4**) upon heating at 88 °C in the solid state or in solution. The rate constant for the rearrangement of **3** to **4** in CD_2Cl_2 solution at 88 °C is $2.9 \pm 0.5 \times 10^{-4}$ s^{-1} ($\Delta G^\ddagger$ = 27.1 ± 0.2 kcal mol^{-1}). Ethylidyne complex $[(C_5H_5)_2(CO)_2Fe_2(\mu\text{-}CO)(\mu\text{-}CCH_3)]^+PF_6^-$ (**10**) gave no detectable isomerization to $[(C_5H_5)_2(CO)_2Fe_2(\mu\text{-}CO)(\mu\text{-}\eta^1,\eta^2\text{-}CH=CH_2)]^+PF_6^-$ (**11**) upon heating at 88 °C for 100 h; at this point, 50% decomposition had occurred ($\Delta G^\ddagger \geq 31$ kcal mol^{-1}). The cyclohexyl substituted carbyne complex $[(C_5H_5)_2(CO)_2Fe_2(\mu\text{-}CO)(\mu\text{-}\overline{CCHCH_2CH_2CH_2CH_2CH_2})]^+PF_6^-$ (**12**) is in rapid equilibrium with the μ-alkenyl complex $[(C_5H_5)_2(CO)_2Fe_2(\mu\text{-}CO)(\mu\text{-}\eta^1,\eta^2\text{-}CH=\overline{CCH_2CH_2CH_2CH_2CH_2})]^+PF_6^-$ (**13**) at ambient temperature ($\Delta G^\ddagger$ = 19.9 ± 0.2 kcal mol^{-1} at −13 °C). The rate of rearrangement of alkylidyne complexes to μ-alkenyl complexes is dramatically accelerated by alkyl substituents on the β carbon of the alkylidyne group. The μ-alkenyl complexes **4** and **13** exhibit a fluxional process which gives rise to a single coalesced cyclopentadienyl resonance at ambient temperature in the ^1H NMR. The barrier for the fluxional process for **4** is 12.9 kcal mol^{-1} and that for **13** is 9.8 kcal mol^{-1} as determined from ^1H NMR coalescence studies. Complex **11** exhibits two resonances for the cyclopentadienyl groups at 27 °C ($\Delta G^\ddagger \geq 14.7$ mol^{-1}). The rates of the fluxional process of the μ-alkenyl complexes and of the rearrangement of μ-alkylidyne complexes are both increased by β-alkyl substitution and indicate increased positive charge at the β-carbon in the transition states for the respective processes.

The diiron methylidyne complex $[(C_5H_5)_2(CO)_2Fe_2(\mu\text{-}CO)(\mu\text{-}CH)]^+PF_6^-$ (**1**) prepared by hydride abstraction from $(C_5H_5)_2(CO)_2Fe_2(\mu\text{-}CO)(\mu\text{-}CH_2)$ (**2**)[1] with $(C_6H_5)_3C^+PF_6^-$ is the first compound in which a C–H unit bridges two metal centers.[2] Although **1** can be stored indefinitely (>6 months) in the solid state at −30 °C, it is extremely reactive toward nucleophiles in solution. For example, alcohols, amines, and CO add to the methylidyne carbon of **1** to form isolable 1:1 adducts.[3] Alkenes such as 1-butene react rapidly with **1** at −50 °C in CH_2Cl_2 to produce μ-alkylidyne complexes such as the μ-pentylidyne complex $[(C_5H_5)_2(CO)_2Fe_2(\mu\text{-}CO)(\mu\text{-}C(CH_2)_3CH_3)]^+PF_6^-$ (**3**); this hydrocarbation reaction proceeds by a regioselective addition of the μ-C—H bond across the C=C bond.[4] Alkylidyne complex **3** can

also be prepared by reaction of $(C_5H_5)_2(CO)_4Fe_2$ with *n*-BuLi followed by acidification with HPF_6.[5] We recently reported that alkylidyne complexes such as **3** rearrange to bridging alkenyl complexes upon heating.[6] The nonequivalent cyclopentadienyl groups of the bridging alkenyl complexes give rise to two separate resonances at low temperature, but a fluxional process interconverts their environment and leads to a single coalesced resonance at ambient temperature. Here we report that the degree of substitution on the β-carbon of the bridging hydrocarbon group has a large effect both on the rate of rearrangement of alkylidyne complexes to bridging alkenyl complexes and on the rate of fluxionality of the bridging alkenyl complexes.

Results

Rearrangement of μ-Alkylidyne to μ-Alkenyl Complexes. When a dilute CD_2Cl_2 solution of pentylidyne complex **3** was heated at 88 °C in a sealed NMR tube for 3.5 h, complete conversion to the bridging alkenyl complex, $[(C_5H_5)_2(CO)_2Fe_2(\mu\text{-}CO)(\mu\text{-}$

(1) Casey, C. P.; Fagan, P. J.; Miles, W. H. *J. Am. Chem. Soc.* **1982**, *104*, 1134.

(2) Subsequently several other μ-methylidyne complexes have been prepared, for example: (a) $\{[(C_5H_5)_2Ru(\mu\text{-}dppm)(\mu\text{-}CO)(\mu\text{-}CH)]^+BF_4^-$ (Davies, D. L.; Gracey, B. P.; Guerchais, V.; Knox, S. A. R.; Orpen, A. G. *J. Chem. Soc., Chem. Commun.* **1984**, 841); (b) $\{(C_5(CH_3)_5)(CO)FeFe(C_5H_5)(CO)\text{-}(\mu\text{-}CO)(\mu\text{-}CH)\}^+PF_6^-$ (Miles, W. H. Ph.D. Dissertation, University of Wisconsin—Madison, 1984); and (c) $\{(C_5H_5)_2(NO)_2Fe_2(\mu\text{-}CH)\}^+PF_6^-$ (Casey, C. P.; Roddick, D. M. unpublished results).

(3) Casey, C. P.; Fagan, P. J.; Day, V. W. *J. Am. Chem. Soc.* **1982**, *104*, 7360.

(4) Casey, C. P.; Fagan, P. J. *J. Am. Chem. Soc.* **1982**, *104*, 4950.

(5) Nitay, M.; Priester, W.; Rosenblum, M. *J. Am. Chem. Soc.* **1978**, *100*, 3620.

(6) Casey, C. P.; Marder, S. R.; Fagan, P. J. *J. Am. Chem. Soc.* **1983**, *105*, 7197.